FROM 3D IMAGING OF STRUCTURES TO DIFFUSIVE PROPERTIES OF ANISOTROPIC CELLULAR MATERIALS

Emmanuel Brun, Jérôme Vicente, Frédéric Topin, Rene Occelli

FROM 3D IMAGING OF STRUCTURES TO DIFFUSIVE PROPERTIES OF ANISOTROPIC CELLULAR MATERIALS

E. Brun, J. Vicente, F. Topin, R. Occelli
IUSTI, Polytech Marseile
5 rue enrico Fermi 13454 Marseille
emmanuel.brun@polytech.univ-mrs.fr

ABSTRACT:
This paper deals with diffusive properties phenomena in metallic foams. We have developed a 3D morphological tool to extract geometrical characteristics of the media from X-ray images. The anisotropy of the geometry of each phase is observed and the relationship between microstructure and effective properties is analyzed. We emphasize on geometrical tortuosity determination and impact on conductive transport tensor. The conductive heat transfers are computed on a vertex-edge network to determine directional effective conductivities by solving the energy equation on this network. We realize a systematic study carried on a wide range of different Nickel foam samples. Finally, we propose a simple model of effective diffusion properties dependence on tortuosity and porosity.

Keywords:
Metallic foams, X-Ray images, morphology, transport properties

1. INTRODUCTION

Metal foams are a new class of materials attractive for numerous applications, as they present high porosity, low relative density, high thermal conductivity of the cell edges and large accessible surface area per unit [1] . Moreover, they also promote mixing and have excellent mechanical properties. Metallic foams are thus used in the field of compact heat exchangers, reformers, biphasic cooling systems and spreaders [2]. Due to their novelty, their complex three-dimensional structure and varied manufacturing processes, metal foams diffusive properties as well as their structural properties are still incompletely characterized.

Thermo-physical and flow properties strongly depend on local morphology of both pores and solid matrix. Local changes of the structure can influence physical properties. Literature models of effective thermal properties, widely used in low porosity media, can no longer be applied to high porosity materials. Most of the modeling approaches are based on arbitrary periodic structures; we propose here to use the real structure[3-5] of the foam from 3D image reconstruction. Several authors have implemented prediction models of effective thermal conductivity of foams.

2. NETWORKS CONSTRUCTION

To take into account of the real geometry of foams we compute several skeletons and we use a node-vertex graph structure in order to easily compute diffusive properties.
We work on a set of Recemat Nickel-Chromium (NC) and (NCX) foam samples. We used cylindrical samples (40mm and 16mm diameter, and thickness 13mm and 6mm). Sample size was maximized in respect with data volume constraint and X-ray images resolution [6].

From binary 3D images (Fluid/Solid voxels) we compute 2 interleaved skeleton. The first one is the network constituted by the interconnected cells (nodes are cells center and edges are links between two adjacent cell). The second one is thin line skeleton of solid matrix (nodes are solid junction and edges are struts).
The goal of the segmentation is to individualize each cell, the method is based the 3D watershed transform [7]. The quality of the cell segmentation depends on the automatic markers extraction. [8] used topographic conditions based on markers neighborhood analysis, but several parameters have to be adjusted depending on the analyzed foam. We improve this method using an automatic marker extraction based on the maximal included ball [9]. We construct an augmented aperture map (both diameter and label of the maximal ball of each voxel). As cells present roughly ellipsoid shape, we suppose that each one contains only one totally included maximal ball. We then keep only one marker by balls, and eliminate redundant markers associated to incomplete balls. Watershed transform is then applied on the pore distance map using the markers extracted as mentioned above.
The fluid network is a bi-partite muli-valuated graph. The two kind of nodes are cells center and throats' barycenter. Throats are identified to voxels, which have 2 different cells in their direct neighborhood. The valuations of edges are the throats' surface, and the edge Euclidean length.
To construct the solid network, we developed a parameter free method based on fluid cell growth using an augmented fast Marching method [10]. Cells' labels are propagated until all voxels are assigned. Voxels in our resulting inflated image are selected according to the Plateau's law. Voxels that have 3 different cells, in their 27 neighbor voxels are edges, and voxels with 4 different cells are nodes. Only nodes are kept to reconstruct the entire solid graph. Labels of adjacent cells are assigned to each node. The solid ligaments are thus obtained by connecting nodes, which have in common at least 3 of their 4 labels.

To study the influence of heat exchanges between the two phases, we interconnect the solid and fluid skeleton on new specific edges and nodes. We connect each throats node to the center of solid edge that delimits this throat.

3. HEAT TRANSFER MODEL

In this approach, we define the effective thermal conductivity tensor of the sample **K** as the constant of proportionality between averaged temperature gradient and averaged heat flux density **q** inside the volume V of the sample [11].

$$\frac{1}{V}\int q(x)dV = -\mathbf{K}\frac{1}{V}\int \nabla T(x)dV \tag{1}$$

Where **K** is a second-order positive symmetric tensor.

This definition requires knowledge of the entire distribution of temperature and heat flux inside the sample. However, the volume integral can be replaced by surface integral [12]. Knowing the geometry of the sample and the distribution of temperature on its surface is therefore sufficient to calculate the average temperature gradient inside the sample. Similarly, the averaged specific heat flux in the x direction is defined by a volume integral. However, integration by parts shows that it can be replaced by a surface integral under steady state conditions. Again, this integral can be easily evaluated knowing the geometry of the sample and measuring the distribution of the fluxes on the boundary of the sample.

$$\bar{q}_x = \frac{1}{V}\left(\int_S x\,\mathbf{q}.\mathbf{n}_x\,dS\right) \tag{2}$$

Heat transfer computation over the solid skeleton allows determining both temperature and heat flux fields over each sample. Radiative transfer between solid surfaces is neglected. Assembling energy balances over all node of the sample lead to a linear system whose unknown are the nodal temperatures. Then heat flux across each strut is deduced from temperature field obtained by solving this linear banded system.

We successively impose along each direction temperature on the two opposite faces and null flux on the four other faces. We can then determine the components of the averaged specific heat flux vector and the components of the averaged temperature gradient for each flux experiment. We obtain a 6 unknown, 9 equations underdetermined system to solve at the least square sense to calculate the thermal conductivity tensor

We observe that the tensor keeps a dominant diagonal. We proceed to full tensor evaluation, but the non-diagonal terms are less than 2% of diagonal one. Thus, calculated values of non-diagonal terms are of same order than estimated numerical error. This is linked to the fact that averaged temperature difference between adiabatic faces is small (~1% of imposed difference).

4. RESULTS

To highlight the angular dependencies of both structural and transport properties, we extract different box-shaped skeletons from the complete sample for different rotations around the z-direction (360 boxes for each sample). For each box we measure thermal conductivity tensor and tortuosity along the three local directions of box. Values along the local X boxes axis are called width-values and thickness-values those along the Z-axis.

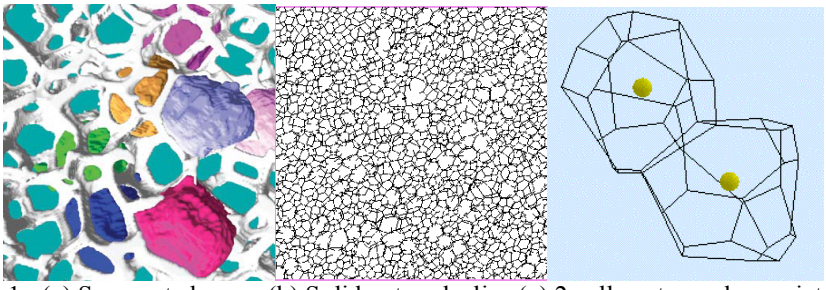

Figure 1.: (a) Segmented pores (b) Solid network slice (c) 2 cell center and associated solid struts

We calculate geometrical tortuosity of each phase from the different graphs with the Dijkstra's algorithm. Edge weights are the Euclidean distance between the two connected vertices. To measure the tortuosity in a given direction (e.g. X-direction), we fix the source vertices at the plane (x0, y, z), and the arrival vertices at the plane (x1, y, z). The tortuosity between the two planes is defined as the arithmetic mean on all the arrival nodes [6]. Thickness tortuosity is independent of rotation while width tortuosity is sinusoidal with a period of 180°. Results show clearly that width solid tortuosity depends on direction and that the solid structure is slightly anisotropic. Similar results are obtained for all foam samples. Width tortuosities are varying into a close range [1.22, 1.42]. There is clearly no relation between tortuosity and pore size.

First we work on the solid phase only. We identify the conductivity according to the three directions corresponding to its opposite faces. The total network length varies slightly with the angle. Knowing the total network length of the boxes and the fixed porosity, we can easily deduce the mean strut section, which is quite independent from the box orientation. As thermal conductivity is proportional to porosity, in order to emphasize on tortuosity effects, we consider that all samples have the same porosity (89.7%). The true porosity values are comprised between 89 and 92. We observe that thickness conductivity as thickness tortuosity is independent on the sample orientation and is greater that width conductivity. Width conductivity variations are significant and correlated to tortuosity variations.

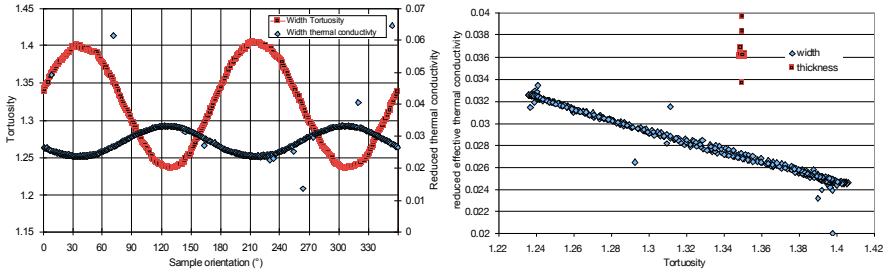

Figure 2.: (a) Directional tortuosity and conductivity (b) Width and thickness conductivity versus tortuosity

Thermal conductivity is inversely proportional to the geometrical tortuosity. We observe a clear linear dependence of width thermal conductivity with tortuosity. Obviously,

conductivity is directly correlated to tortuosity in the width of the sample. But in the thickness, we obtain for a given tortuosity ~1.35 a different value of conductivity. For all foam samples, the same linear dependences relies the width tortuosity and the width conductivity. Nevertheless, tortuosity is not the only geometrical parameter driving the effective thermal conductivity because for a given tortuosity two different conductivity values are obtained for the thickness and the width direction. Predicted effective conductivity of solid phase has already been compared to experimental data with a very good agreement [6].

We evaluate influence of fluid conduction and fluid-solid heat exchange on effective conductivity. Indeed using the network approach is fully justified as the solid phase is constituted of ligaments. Fluid phase topology is clearly different from the network one. Assimilating heat transfer on the fluid phase to monodimensional heat transfer on the fluid network is, indeed, a strong approximation. On the same way, to locate interphase heat exchanges only at nodes will limit the representativity of results. Anyway, the qualitative behavior will be captured.

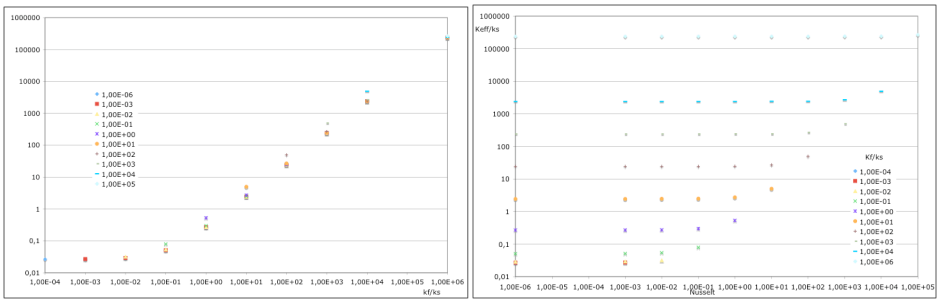

Figure 3.: Influence of (a) fluid conductivity and (b) Nusselt number on effective conductivity

Clearly fluid phase and heat exchange networks behave in parralel network to the solid graph. For a given fluid conductivity, Nusselt number (non-dimensional heat exchange coefficient) has a weak influence on global effective conductivity as expected for diffusive behavior of both phases.

5. CONCLUSION

The effective thermal conductivity tensor is identified. It helps understanding heat transfers in the foam and how they are correlated to the local structure. This constitutes an important step to the prediction of the conductivity tensor of the foam from its real structure. However, this work is not yet a fully quantitative prediction method of conductivity tensor values. A systematic study of the impact of morphology on transport properties has been presented with different samples of different textures. We developed a morphological analysis tool to quantify the main structural parameters of metallic foams. It provides the functions of geometrical measurements (specific area, pore size distribution...). Cell shapes are measured and specific cell orientations are quantified. An original method based on graph theory has been developed to measure the geometrical tortuosity of solid phases. Anisotropy of the solid matrix is observed. The tortuosity

measurements carried out for different directions in the sample show a clear correlation between tortuosity values and effective thermal conductivity. An efficient skeletization method gives the vertex-edge graph of the both phases. The identification of nodes, segments, and connectivity of the graphs has been carried out. We have been able to calculate heat fluxes and temperature gradients by solving the energy equation within these network. A direct numerical simulation is under investigation to complete this network approach and is expected to allow to define a fully representative fluid heat transfer network.

References

[1] Ashby, M.F., et al., *Metal foams: A design guide* 2000, Boston, MA: Butterworth – Heinemann.

[2] Tadrist, L., et al., *About the Use of Fibrous Materials in Compact Heat Exchangers*. Experimental Thermal and Fluid Science, 2004. **28**: p. 193 – 199.

[3] Boomsma, K. and D. Poulikakos, *On the effective thermal conductivity of a three-dimensionally structured fluid-saturated metal foam*. International Journal of Heat and Mass Transfer 2001. **44**: p. 827-836.

[4] Calmidi, V.V. and R.L. Mahajan, *The effective thermal conductivity of high porosity fibrous metal foams*. Journal of Heat Transfer, 1999. **121**: p. 466-471.

[5] Bhattacharya, A., V. Calmidi, and R.L. Mahajan, *Thermophysical properties of high porosity metal foams*. Int. J. Heat Mass Transfer, 2002. **45**(5): p. 1017-1031.

[6] Vicente, J., et al. *Thermal conductivity of metallic foam: simulation on real x-ray tomographied porous medium and photothermal experiments* in *IHTC13, 13TH International Heat Transfer Conference*. 2006. Sydney.

[7] Meyer, F. and S. Beucher, *Morphological segmentation*. Journal of Visual Communication and Image Representation, 1990. **1**(1): p. 21-46.

[8] Dillard, T., et al. *In-situ observation of tensile deformation of open-cell nickel foams by means of X-ray microtomography* in *3rd International Conference on Cellular Metals and Metal Foaming Technology (MetFoam 2003*. 2003. Berlin (Germany).

[9] Beucher, S. *Numerical residues*. in *7th International Symposum on Mathematical Morphology*. 2005. Paris.

[10] Sethian, J.A., *Level Set Methods and Fast Marching Methods*. 1999, Cambridge, UK, : Cambridge University Press.

[11] Rubin, Y. and J. Gomez-Hernandez, *A stochastic approach to the problem of upscaling of conductivity in disordered media: Theory and unconditional numerical simulation*. Water Resources Res, 1990. **22**(4): p. 691-701.

[12] Sanchez-villa, X., J.P. Girardi, and J. Carrera, *A synthesis of approaches to upscaling of hydraulic conductivities*. Water Resources Res, 1995. **31**(4): p. 867-882.